Fabrication of hollow molecularly imprinted polymer for selective adsorption of amoxicillin

Lingli Li[a], Ang Li[a], Peilin Yu[a], Xudong Zheng[a,b,*], Hongxiang Ou[a,b,]*

[a]*School of Environmental and Safety Engineering, Changzhou University, Changzhou 213164, China, email: zhengks@outlook.com*
[b]*Jiangsu Engineering Research Center of Petrochemical Safety and Environmental Protection, Changzhou 213164, China*

ABSTRACT

The structurally stable molecularly imprinted hollow microspheres (MIHM) were prepared by the Pickering emulsion method using ZIF-8 as the stable particle and amoxicillin (AMOX) as the template molecule. MIHM were used to separate amoxicillin from solution. The physicochemical properties and adsorption properties of MIHM were studied by scanning electron microscope, Fourier transform–infrared spectroscopy and X-ray diffraction and static adsorption experiments. The results show that ZIF-8 nanoparticles can stabilize the Pickering emulsion, and the particles are distributed on the surface of hollow MIHM capsules with a capsule size of about 20–80 μm. The results of adsorption experiments showed that MIHM had a large adsorption capacity for AMOX, and reached an adsorption capacity of 0.1577 mmol g^{-1} in AMOX solution (308 K, pH = 7.0, and 100 mg L^{-1}). MIHM showed high selectivity for AMOX in selective adsorption experiments. After 5 cycles of recycling, the adsorption capacity of materials only decreased by 9.03%. So, it proves that the MIHM have good regenerability.

Keywords: Amoxicillin; Molecular-imprinted; Selective adsorption; Pickering emulsion

1. Introduction

Antibiotics have been widely used in medical, animal husbandry, agriculture and other industries in recent years. Most of the antibiotics are discharged into the environment through human and animal excreta, agricultural and sewage in the form of original drugs or metabolites [1]. It has long-term existence in the natural environment through sedimentation and bioaccumulation, which has a chronic toxic effect on the organism [2]. Antibiotic wastewater generally has the characteristics of complex composition and difficult biodegradation. The removal of antibiotic residues in water has always been one of the hot spots of environmental water resource protection. In the existing treatment methods, precipitation filtration and biological treatment are inefficient [3], and electrochemical method [4], advanced oxidation method [5] and membrane technology [6] are complicated and costly, and further research and improvement are needed and provide a wide range of applications. Adsorption is a simple and efficient physicochemical separation method, which has been proved to be an important means of water treatment in many fields [7–9]. At the same time, the adsorption method shows obvious advantages in removing antibiotics, and it is considered one of the most promising methods. Various adsorbents such as activated carbon, carbon nanotubes, graphene, zeolite, chitosan, and resins can be used to adsorb antibiotics in water [10]. Zhu et al. [11] prepared erythromycin molecularly

* Corresponding authors.

imprinted material for adsorption of erythromycin in water based on magnetic eggshell-stabilized Pickering emulsion polymerization. The results showed that the adsorption rate of erythromycin was over 70%.

The enrichment of antibiotics in water by absorbent is an effective and green research direction. In recent years, molecularly imprinted technology (MIT) [12,13] has been widely used in the fields of electrical sensing detection and chromatographic separation [14]. It is a technology for preparing polymers with specific recognition properties for template molecules. The molecular imprinting technology has poor stability and good adsorption selectivity [15]. The combination of molecular imprinting technology and high stability materials, and the combination of high selectivity of molecular imprinting technology and high adsorption materials, complement each other, adsorbents with good application prospects will be prepared. Metal-organic framework materials (MOFs) are porous materials composed of inorganic metal centers (metal ions or metal ion clusters) and organic ligands [16]. They have attracted much attention in recent years because of their huge porosity, flexible pore structure and easy functionalization [17]. Combining porous metal-organic framework materials with molecular imprinting techniques by means of Pickering emulsions, which stabilizes the formation of oil-in-water or water-in-oil emulsions [18], MOFs materials such as ZIFs with oil-water amphiphilic also ensures the feasibility of the combination [19,20].

In this study, molecular imprinting techniques were combined with metal-organic framework materials via Pickering emulsions. ZIF-8 was used as emulsion stabilizing particles, and amoxicillin (AMOX) was used as a template molecule to prepare molecularly imprinted hollow microspheres (MIHM) for selective adsorption separation of AMOX in solution. To study the properties and performances of MIHM by characterizing and static adsorption experiments.

2. Experimental

2.1. Materials

Zinc nitrate [$Zn(NO_3)_2 \cdot 6H_2O$, 99%], amoxicillin (AMOX·$3H_2O$), tetracycline (TCY, 98%), ergotamycin (EM, 98%), 2-methylimidazole (99%), styrene (99%), divinylbenzene (DVB, 80%), dodecane (99%), APTEs, (95%), and azobisisobutyronitrile (AIBN, 97%) were purchased from Aladdin Reagent Co., Ltd., (Shanghai, China). Acetic acid, ethanol, methanol, and sodium hydroxide (NaOH) were obtained from Sinopharm Chemical Reagent Co., Ltd., (Shanghai, China). Aqueous mixed film (25 mm/0.22 μm) were purchased from Rebs Flagship Store (Shanghai, China). All experiments using deionized water (DW). Scanning electron microscope (SEM, JEOL, Japan), Fourier transform–infrared spectrophotometer (FT–IR, IS50, United States), thermogravimetric analyzer (Q600-TGA/DSC, United States), Rigaku D/max 2500 VL diffractometer (Japan).

2.2. Characterization

The Pickering emulsion obtained in the experiment was observed by using an optical microscope. (Phenix, Jiangxi, China). The discrete phase was mixed by a shear force instrument (Lankier, Shanghai, China). The SEM presentations of MIHM were viewed using JSM-7001F (JEOL Ltd., Japan). The size distribution of MIHM was analyzed by a granulometer (Winner, Jinan, China). The pH/mV instrument (PHS-3C, Xi'an, China) was used to adjust the pH of the solution during the experiment. The Nicolet NEXUS-470 FT–IR apparatus (Thermo, America) was used for the recording of Fourier transform–infrared absorption spectroscopy. The zeta potential of MIHM in an aqueous solution was measured with Zeta potential measurement (ZEN3600, Malvern Instruments, England).

2.3. Synthesis of ZIF-8 nanoparticles

Initial efforts focused on preparing ZIF-8 to ensure its stability at oil-water interfaces. Finally, we identified the following sustainable and reliable methods. ZIF-8 nanoparticles were synthesized according to previous literature with minor modification as follows [21,22]: Accurately weight 0.59 g of zinc nitrate hexahydrate and 11.35 g of 2-methylimidazole separately into 40 mL of deionized water, followed by mixing with strong stirring (1,000 rpm) for 1 h at room temperature, and the mole rate of 2-methylimidazole to zinc was 70:1. The nanoparticles were collected by repeated centrifugation (4,000 rpm, 0.5 h) and washed thrice by DW. The final product was air-dried for the preparation of hollow microspheres.

2.4. Synthesis of the molecularly imprinted polymer on ZIF-8@polystyrene (MIHM)

The preparation of MIHM was referenced and improved as follows [23,24]: At first, 15.2 mg of amoxicillin and 60 μL of APTEs (3-aminopropyl triethoxy silane) were mixed in 10 mL of DW with 1 h oscillation for pre-assembly. Then, 0.20 g of ZIF-8 particles were dispersed in it by ultrasound for 10 min to form the aqueous phase. AIBN at 0.0078 g was dissolved in 0.14 g of styrene, 0.21 g of divinylbenzene (DVB), and 0.40 g of dodecane to form the oil phase, which was subsequently mixed with the water phase in a 25 mL beaker. A stable O/W Pickering emulsion was prepared by means of a shear device at a speed of 15,000 rpm and stirring for 2 min. The resulting emulsion was poured into a 100 mL flask, equipped with a cooling condenser, and N_2 was introduced into it for 20 min. The reaction mixture was then heated to 348 K, followed by polymerization at this temperature for 16 h. The final product was isolated via filtration, added with ethanol to wash with a centrifuge at 1,000 rpm for 1 min, the material was repeatedly eluted with a mixture of methanol/acetic acid (9:1, v v^{-1}) until the presence of template molecules was no longer detected in the eluate, then washed with pure ethanol and finally dried in air for 12 h. For comparison, NIP/ZIF-8@PS were prepared in a parallel procedure but without the adjunction of AMOX, while ZIF-8@PS without the AMOX and APTEs, this article calls it NIHM. MIHM and NIHM are made of self-assembled film added during the synthesis process, and HM is made of self-assembled film added during the synthesis process.

2.5. Adsorption experiments

The static adsorption experiment included the influence of parameters such as initial pH, contact time, temperature and initial concentration of AMOX on the adsorption performance. The dosage of the adsorbent was 0.5 g L^{-1}. Add MIHM to a solution (20 mL) of AMOX at a concentration ranging from 10 to 100 mg L^{-1}, then sealed and suspended at different temperatures (respectively, 288 K, 298 K and 308 K) and mixed in a stirring tank with 200 revolutions for 12 h. MIHM and the solutions were separated by an inorganic filter membrane, and the amount of AMOX in the colatuie was determined by the UV–Vis spectrophotometry (UV-1901, Xipu, Shanghai, China) at 231 nm. The batch kinetics study was carried out in the same manner as the adsorption experiment with the AMOX concentration of 100 mg L^{-1}, but the aqueous samples were obtained at predetermined time intervals. The amount of AMOX adsorbed at the time (t) was calculated by the mass balance Eq. (1).

$$Q_t = \frac{1,000(C_0 - C_t)V}{WM}$$

(1)

where, Q_t (mmol g^{-1}) represents the absorption of AMOX; C_0 (mmol L^{-1}) represents the initial concentration of the AMOX; C_t (mmol L^{-1}) refers to the concentration at which the AMOX in the water reaches equilibrium; V, W and M are the volume (L) of the solution, the mass of the adsorbent (mg) and the molecular weight of AMOX, respectively.

2.6. Adsorption selectivity

The selectivity of MIHM cavities was performed using two different antibiotics, commonly employed in the medical industry and animal husbandry, and the rebinding percentage of each antibiotic to the polymer was compared to that of AMOX. The antibiotics used in this study were erythromycin (EM) and Tetracycline (TCY).

2.7. Regeneration of adsorbent

Add 5 mg MIHM to 20 mL of 100 mg L^{-1} AMOX solution and adsorb for 12 h at 308 K, the concentration of AMOX was measured by ultraviolet spectrophotometer. After 8 h of vacuum drying at 313 K, the desorbed and regenerated MIHM was repeated and the concentration of AMOX in the adsorbed and regenerated MIHM was determined. The adsorption performance of the regenerated MIHM was studied by five times during adsorption–desorption process.

3. Results and discussion

3.1. Characterization of MIHM

In this study, a stable O/W Pickering emulsion Fig. 1a is one of the most important steps in preparing MIHM. According to Fig. 1a, some oil-in-water microemulsion ranging from 20 to 100 μm can be observed, which is consistent with the subsequent molding sample. In Fig. 1b, the ZIF-8 nanoparticles are observed by the SEM, and it shows a good hexahedron structure.
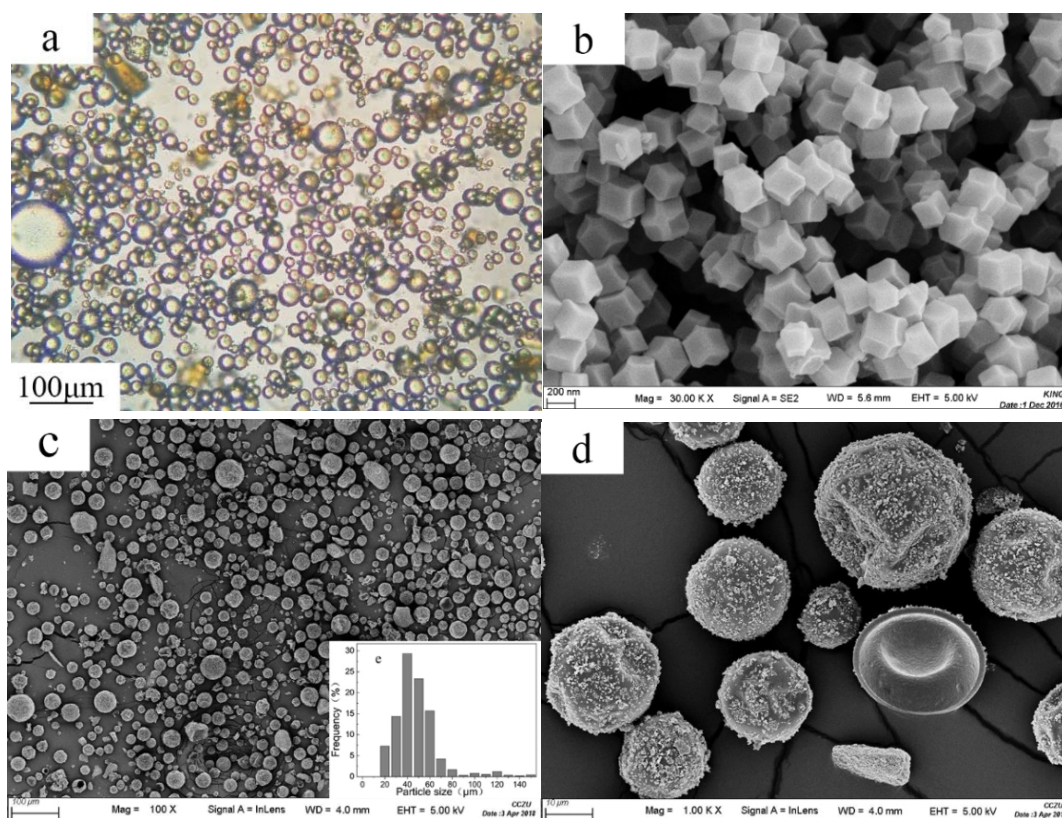

Fig. 1. Pickering emulsion micrograph (a) SEM of ZIF-8 and (b) SEM of MIHM (c)–(d).

The hollow structure is formed with the preparation of the oil-in-water emulsion. After the thermal polymerization, the oil phase formed a polyethylene polymerization layer covering with nano-ZIF-8 particles. The polymerization layer ensures the stability of the hollow structure, and the exposed ZIF-8 particles on the layer provide a highly effective adsorbing surface for the sample. The hollow structure of the MIHM can be observed from Fig. 1c–d, and the surface of MIHM is covered with ZIF-8 nanoparticles. The size and distribution of MIHM are shown in Fig. 1c.

It is showed that the size of MIHM ranges from 20 to 80 μm. Fig. 1d shows the cross-section of MIHM clearly which proves MIHM is hollow. The cross-section of the microspheres in Fig. 1d shows that the inner part of the microspheres is smooth and the outer surface is unsmooth obviously (ZIF-8 and imprinting layer). All these results indicate that the imprinted loading part and ZIF-8 are mainly distributed on the surface of the capsules and the structure is hollow.

It was characterized using FT–IR for the composition sample for each sample: MIHM, HM and NIHM. Fig. 2 shows the FT–IR of MIHM, HM and NIHM. From the analysis of the graph, the infrared absorption curves of the three samples are same. The MIHM and NIHM of APTEs added during the synthesis process have the stretching vibration (vertical solid line) of the unique Si–O–Si of APTEs at $1,065 \text{ cm}^{-1}$, The HM without APTEs added during the synthesis was significantly different from the other two samples. The results show that APTEs as functional monomers have been successfully combined with hollow capsules through pre-polymerization and other synthetic processes.

Fig. 3 shows the X-ray diffraction (XRD) curves of ZIF-8, MIHM and NIHM. The XRD curves of MIHM and NIHM fit well with the crystal curves of ZIF-8 nanoparticles. The typical characteristic peaks of MIHM and NIHM in 011, 002, 112, 022, 013 and 222 are similar to ZIF-8 crystals, and the other impurity peaks are not obvious. It shows that the prepared MIHM has only high crystallinity ZIF-8 crystals. The peak value of ZIF-8 particles is higher than that of MIHM, indicating that the abundance of MIHM decreases with the formation of the polymer layer.
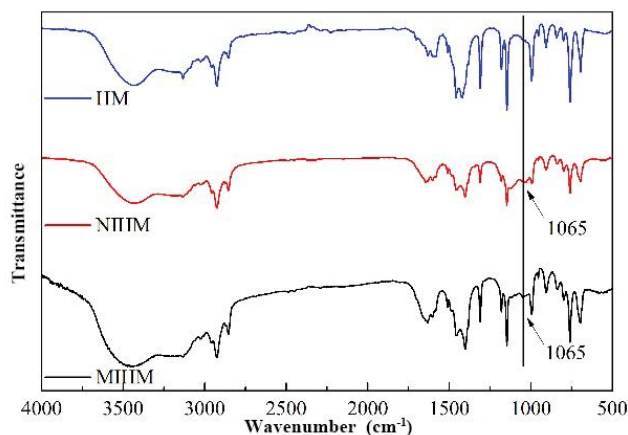
3.2. Effect of pH

The initial pH of the solution is the most important factor affecting the adsorption performance of the adsorbent on amoxicillin. This is because the surface charge of amoxicillin ionized varies with the pH of the solution. The change in the ionization state of the amoxicillin molecule is caused by the ionization of the carboxyl group (pKa1 = 2.68), the amino group (pKa2 = 7.49) and the phenolic hydroxyl group (pKa3 = 9.63). Therefore, AMOX with an initial pH range of 4.0 to 10.0 and a concentration of 100 mg L^{-1} was selected to study the effect of different pH values on the adsorption of amoxicillin. The zeta potential of the adsorbent at different pH conditions was also measured. Fig. 4 shows that the adsorption content of adsorbent increases from 0.0456 to $0.1526 \text{ mmol g}^{-1}$ and the Zeta potential of adsorbent solution decrease from 5.28 to 1.94 mV when the initial pH of the solution increases from 4.0 to 7.0. The adsorption capacity of adsorbents in different initial pH solutions is mainly related to Zeta potential and the dissociation of adsorbents. When the pH is less than 7.0 because MIHM and AMOX both contain $-NH_2$ and $-NH_3^+$ in acidic solution, The zeta potential of MIHM is mainly characterized by the fact that the positive potential is repulsive with AMOX [25,26]. When the pH increased, that is, the pH is 7.0–10.0, the content of $-NH_3^+$ in MIHM and AMOX decreased, and the adsorption capacity of MIHM increased gradually until a relatively balanced capacity was reached.

3.3. Adsorption isotherm

Adsorption isotherms are used to study the specific relationship between the adsorbed materials and adsorbent surface. The adsorption capacity of MIHM to AMOX solution with a pH of 7.0 at a concentration of $10–100 \text{ mg L}^{-1}$ at three different temperatures of 298 K, 308 K and 318 K was determined and fitted by Langmuir and Freundlich models. The Langmuir model assumes that adsorption is performed on a single homogeneous
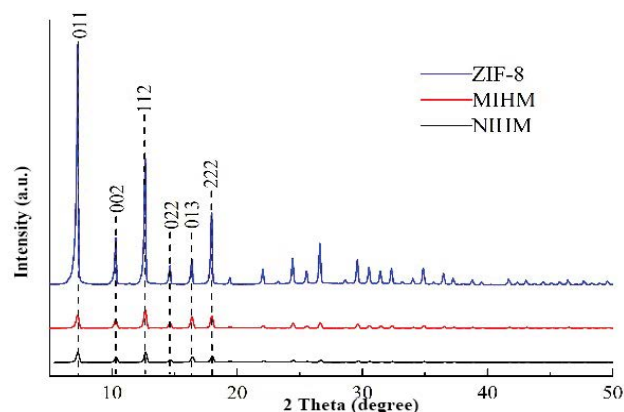

Fig. 2. FT–IR curves of MIHM, NIHM and HM.

Fig. 3. XRD curves of ZIF-8, MIHM and NIHM.

surface and that the energy of all binding sites is uniform. Freundlich equation is an empirical model, it is assumed in the non-uniform surface adsorption is reversible. The Langmuir and Freundlich model are represented by the following nonlinear Eqs. (2) and (3):

$$Q_e = \frac{K_L Q_m C_e}{1 + K_L C_e} \tag{2}$$

$$Q_e = K_F C_e^{1/n} \tag{3}$$

where K_L (L mmol^{-1}) is the Langmuir adsorption equilibrium constant, and K_F (mol L g^{-2}) is the Freundlich adsorption equilibrium constant. Larger K_F value indicates a larger amount of adsorption, while $1/n$ is an indicator of exchange strength or surface heterogeneity, with $1/n$ being less than 1.0, indicating good removal conditions. In order to predict the advantages of the adsorption system, the affinity constant R_L can also be used for the representation of the Langmuir model, which is defined as follows:

$$R_L = \frac{1}{1 + C_m K_L} \tag{4}$$

Among them, C_m represents the initial concentration of the target adsorbent AMOX. R_L represents the affinity and adsorption performance of the adsorption system. When $0 < R_L < 1.0$, the adsorption performance is good.

As shown in Table 1, the adsorption fitting constants of both models and MIHM are higher. Combined with the convex adsorption isotherm shown in Fig. 5 and the adsorption mechanism of the adsorbent itself, it can be known that the Langmuir model is more suitable for describing the adsorption process. Under three different temperatures, R_L was less than 1.0, which indicated that MIHM had good adsorption performance. Good fitting with Langmuir ensures further analysis of MIHM imprinted load performance. When the temperature rises from 298 K to 318 K, the adsorption capacity of MIHM to AMOX increases. Detailed analysis of the adsorption capacity is presented in the thermodynamic analysis section.

The adsorption isotherm of NIHM for AMOX was determined at 318 K under the same experimental conditions. The imprinting factor (I) is calculated by fitting results. The imprinting factor is a good method to evaluate the properties of imprinted polymers. The parameters are calculated by the fitting coefficient K_L of the Langmuir model. The expression formula for the value of I is as follows:

$$I = \frac{K_{L,\text{MIP}}}{K_{L,\text{NIP}}} \tag{5}$$

When the imprinting factor I is greater than 1.0, the effect of imprinting load is better. As shown in Fig. 6, at 318 K, the I value is 4.1884, which is greater than 1.0,

indicating that the MIHM imprinting selection cavity has a strong ability to combine with AMOX.

3.4. Adsorption kinetics

The research contents of adsorption kinetics include adsorption and desorption rate, transformation, and so on. It can be better studied by fitting the adsorption kinetics model. Adsorption kinetics of MIHM was studied under 318 K. The initial solution concentration of AMOX was 100 mg L^{-1} from 0 min to 720 min. The experimental process and data were fitted and analyzed by quasi-first and quasi-second order kinetic adsorption equations. The expressions of the two Eqs. (6) and (7), respectively.

$$Q_t = Q_e - Q_e^{(-k_1 t)} \tag{6}$$

$$Q_t = \frac{k_2 Q_e^2 t}{1 + k_2 Q_e t} \tag{7}$$

Among them, the adsorption amount and equilibrium adsorption amount at time t are Q_t (mmol g^{-1}) and Q_e (mmol g^{-1}), k_1 (1 min^{-1}) and k_2 [g·(mmol min)$^{-1}$] are respectively pseudo-first and second-order rate constants.

As shown in Fig. 7, the adsorption kinetic data of MIHM increased rapidly within the first 60 min and achieved 69.24% of the balancing capacity and then increased slowly until reaching the equilibrium after 3.0 h. The adsorption capacity of MIP was achieved at 0.1413 mmol g^{-1}. The pseudo-first-order model has a better fit ($R^2 = 0.9917$), which is more suitable for adsorption data, and the adsorption rate is extremely fast, indicating that the physical interaction may be related to adsorption.

3.5. Adsorption thermodynamics

Thermodynamics is to study the properties of the material system in equilibrium and establish the energy balance relationship, including the interaction between the system and the outside world and the energy transfer and transformation when the state changes. Thermodynamic parameters of adsorption process are calculated by equation ΔG (8), ΔH and ΔS (9):

$$\Delta G = -RT \ln K_0 \tag{8}$$

$$\ln K_0 = \frac{\Delta S}{R} - \frac{\Delta H}{RT} \tag{9}$$

where ΔG (kJ mol^{-1}) is Gibbs free energy, ΔH (kJ mol^{-1}) is standard enthalpy ΔS [J (mol K)$^{-1}$] is entropy change. T (K) is thermodynamic temperature, R [8.314 J (mol K)$^{-1}$] is the ideal gas constant, K_0 is the thermodynamic equilibrium constant.

From Table 2 we can see that ΔG is negative, which indicates that the process of MIHM adsorbing AMOX is spontaneous. With the increase of temperature, the ΔG value

increases, which indicates that the higher the temperature is, the greater the amount of AMOX adsorbed by MIHM. The standard adsorption enthalpy ΔH of MIHM for AMOX is positive, which further confirms that the adsorption process is internal heat and physical adsorption. In general, the positive value of H further confirms that the adsorption process is endothermic and physically adsorbed. These findings are consistent with the obtained isotherms. The positive value of S indicates the randomness of the increase at the solid-solution interface. As the temperature increases, the increase in AMOX adsorption may also be caused by the rate of increase of the particles.

3.6. Adsorption selectivity

Fig. 9 shows that the adsorption capacity of NIHM on three antibiotics is lower than that of MIHM, and there is little difference between them. This indicates that NIHM has fewer sites for adsorption and lacks imprinted holes. The adsorption capacity of MIHM on template molecule

AMOX is larger than that of the other two substances. The adsorption capacity of MIHM on AMOX, TCY and EM are 0.1548, 0.0624, 0.0391 mmol g⁻¹, which proves that MIHM can selectively adsorb AMOX. The adsorption capacity of TCY, a structural analogue of template molecule AMOX, was higher than that of EM, and the adsorption capacity of TCY increased after imprinting. The results show that the characteristics of imprinted holes can also identify the structural analogues of template molecules.

3.7. Reusability of the ZIF-8@PS

Five experiments of adsorption–desorption cycle regeneration of MIHM were carried out. The results of the experiments are shown in Fig. 10. After one, two, three, four and five cycles, the saturated adsorption capacity of MIHM to the initial temperature 318 K, initial concentration 100 mg L⁻¹ AMOX solution was 0.1500, 0.1486, 0.1452, 0.1416 and 0.1409 mmol g⁻¹, respectively. After five cycles, the loss rate of saturated adsorption capacity was only 9.03%. For comparison, the saturated adsorption
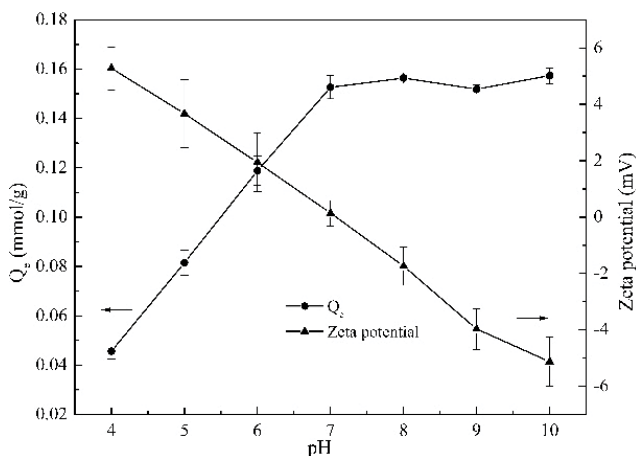

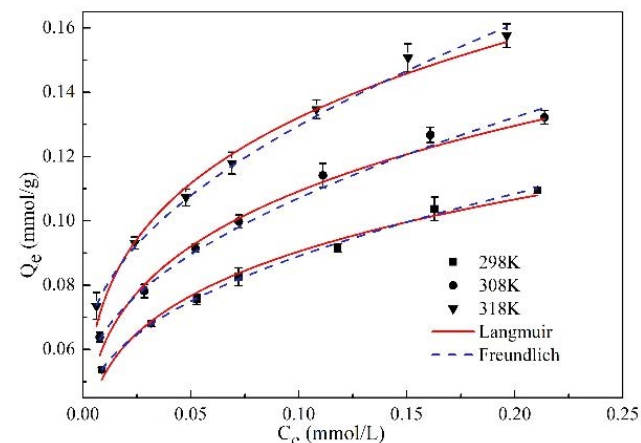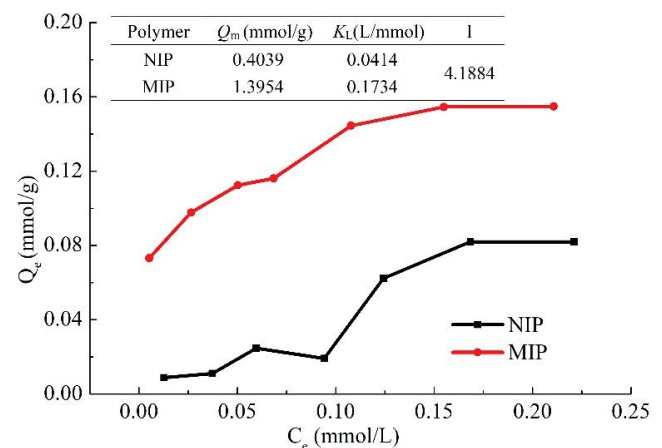Fig. 4. Effect of solution pH on MIHM adsorption capacity.

Fig. 6. Data and fitting parameters of MIHM and NIHM adsorbing different concentrations of AMOX under 318 K conditions.

Fig.5. AMHM data and its fitting curve of MIHM adsorbed at different temperatures.
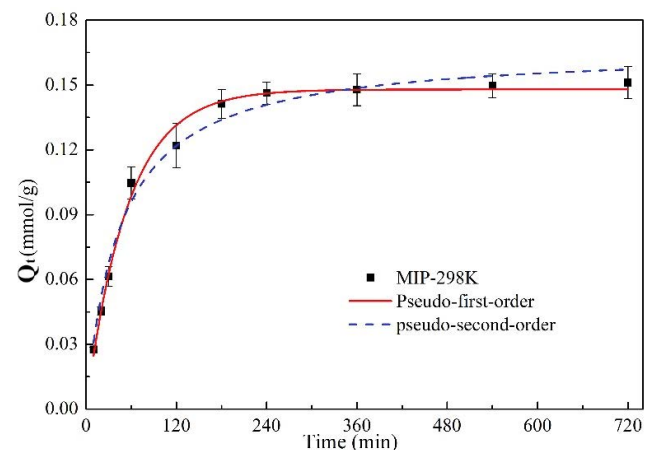

Fig. 7. Kinetic data and modeling for the adsorption of AMOX onto MIP at 298 K (the initial concentration of 100 mg/L).

Table 2
Adsorption of AMHM data and its fitting curve at different temperatures

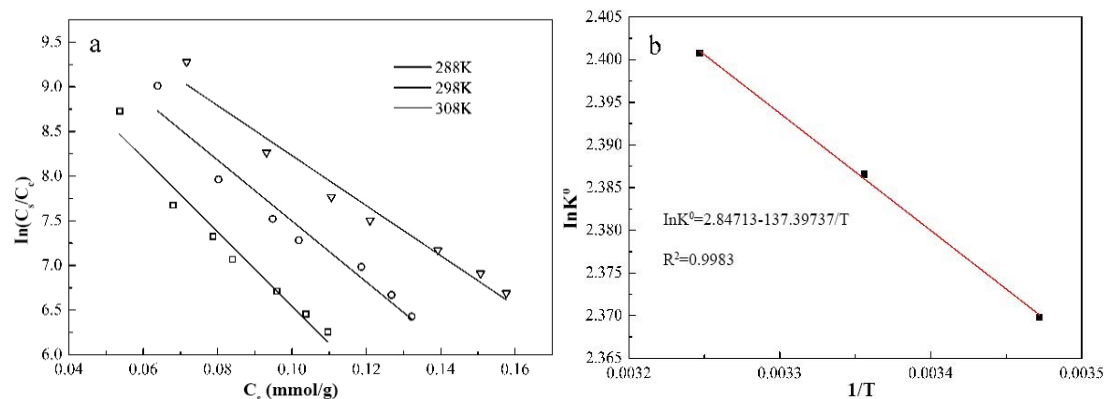| T (K)	Langmuir model				Freundlich model		
	Q_m (mmol g^{-1})	K_L (L mmol^{-1})	R^2	R_L	K_F (mmol g^{-1})	$1/n$	R^2
288	1.3824	0.1307	0.9536	0.9698	0.1750	0.2805	0.9542
298	0.7996	0.3513	0.9941	0.9227	0.2425	0.3193	0.9998
308	1.3954	0.1734	0.9587	0.9931	0.2799	0.3835	0.9719

Fig. 8. Thermodynamic data and fitting of MIHM adsorption.

Table 3
Thermodynamic parameters of MIHM adsorption AMOX

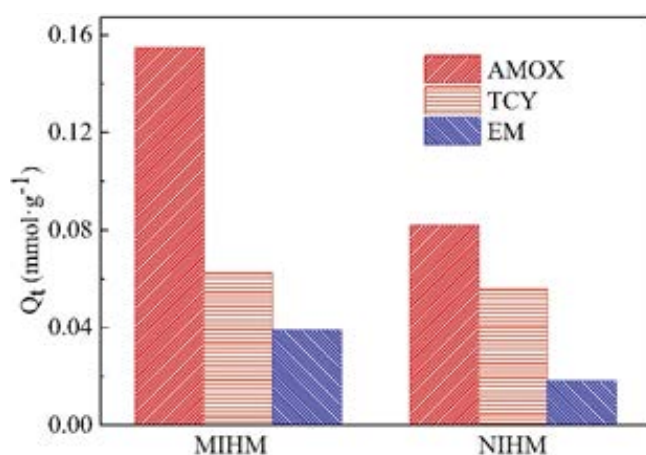| Temperature (K)	$\ln K_0$	ΔG (kJ mol^{-1})	ΔH (kJ mol^{-1})	ΔS [J (mol K)$^{-1}$]
298	2.369	−5.871		
308	2.387	−6.111	1.142	0.0237
318	2.401	−6.347		

Fig. 10. Recycled adsorption results of MIHM.

Fig. 9. Selective adsorption results of MIHM and NIHM.

capacity of activated carbon for AMOX under the same conditions is only 0.1248 mmol g^{-1} [27]. The results show that MIHM has good regeneration performance, and reuse has little effect on imprinted voids and surfaces.
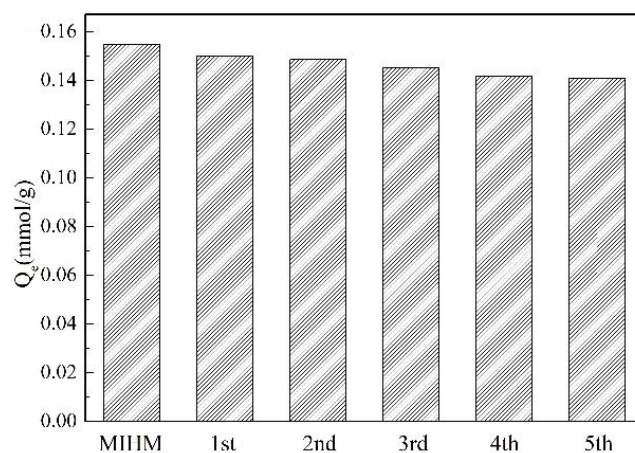
4. Conclusions

In this study, Pickering emulsion method combined with ZIF-8 and molecularly imprinted technology was used to prepare a stable structure and imprinted holes adsorption material. Through a series of characterization, the excellent adsorption performance and imprint performance of MIHM were proved, and the adsorption data were obtained through a series of static and dynamic adsorption experiments. The experimental results show that the material has a hollow structure, imprinting is loaded on the outside of the capsule and the load is good. In static adsorption experiments, the isothermal adsorption of MIHM fits well with the Langmuir model and tends to be monolayer

adsorption. At 318 K, the maximum adsorption capacity of MIHM was 0.1577 mmol g^{-1}. Adsorption kinetics and thermodynamics proved that the adsorption of AMOX by MIHM belongs to physical adsorption and the process is endothermic. MIHM has a good imprinting load. Compared with NIHM, MIHM has a better adsorption performance and excellent selective recognition for AMOX. After five times of adsorption and desorption, the loss rate of adsorption capacity of MIHM is 9.07%, which can be effectively regenerated.

References

[1] A. Christou, A. Agüera, J.M. Bayona, E. Cytryn, V. Fotopoulos, D. Lambropoulou, C.M. Manaia, C. Michael, M. Revitt, P. Schröder, D. Fatta-Kassinos, The potential implications of reclaimed wastewater reuse for irrigation on the agricultural environment: the knowns and unknowns of the fate of antibiotics and antibiotic resistant bacteria and resistance genes – a review, Water Res., 123 (2017) 448–467.

[2] M.A.E. de Franco, C.B. de Carvalho, M.M. Bonetto, R. de Pelegrini Soares, L.A. Féris, Removal of amoxicillin from water by adsorption onto activated carbon in batch process and fixed bed column: kinetics, isotherms, experimental design and breakthrough curves modelling, J. Cleaner Prod., 161 (2017) 947–956.

[3] C. Huang, M.-T. Luo, X.-F. Chen, L. Xiong, X.-M. Li, X.-D. Chen, Recent advances and industrial viewpoint for biological treatment of wastewaters by oleaginous microorganisms, Bioresour. Technol., 232 (2017) 398–407.

[4] O. Sahu, Performance of copper compounds in chemical and electro oxidation treatment of sugar industry waste water: batch reaction, J. Taiwan Inst. Chem. Eng., 65 (2016) 256–268.

[5] S.Y. Jasim, J. Saththasivam, Advanced oxidation processes to remove cyanotoxins in water, Desalination, 406 (2017) 83–87.

[6] I. Bae, K.-H. Oh, S.-H. Yun, H. Kim, Asymmetric silica composite polymer electrolyte membrane for water management of fuel cells, J. Membr. Sci., 542 (2017) 52–59.

[7] A. Sapienza, A. Velte, I. Girnik, A. Frazzica, G. Füldner, L. Schnabel, Y. Aristov, "Water - Silica Siogel" working pair for adsorption chillers: adsorption equilibrium and dynamics, Renewable Energy, 110 (2017) 40–46.

[8] M. Fechtner, A. Kienle, Efficient simulation and equilibrium theory for adsorption processes with implicit adsorption isotherms – mass action equilibria, Chem. Eng. Sci., 171 (2017) 471–480.

[9] Y.-z. Zhang, T.-t. Bian, Y. Zhang, X.-d. Zheng, Z.-y. Li, Effective and green tire recycling through microwave pyrolysis, J. Zhejiang Univ.-Sci. A, 19 (2018) 951–960.

[10] Q. Chen, Preparation of molecularly imprinted adsorbent materials and study on the properties of separation/enrichment antibiotics, 2016.

[11] Y.Z. Zhu, D.Y. Jiang, D.S. Sun, Y.S. Yan, C.X. Li, Fabrication of magnetic imprinted sorbents prepared by Pickering emulsion polymerization for adsorption of erythromycin from aqueous solution, J. Environ. Chem. Eng., 4 (2016) 3570–3579.

[12] R. Sedghi, B. Heidari, M. Yassari, Novel molecularly imprinted polymer based on β-cyclodextrin@graphene oxide: synthesis and application for selective diphenylamine determination, J. Colloid Interface Sci., 503 (2017) 47–56.

[13] H.R. Ali, H.H. El-Maghrabi, F. Zahran, Y.M. Moustafa, A novel surface imprinted polymer/magnetic hydroxyapatite nanocomposite for selective dibenzothiophene scavenging, Appl. Surf. Sci., 426 (2017) 56–66.

[14] G.M. Yang, F.Q. Zhao, Molecularly imprinted polymer grown on multiwalled carbon nanotube surface for the sensitive electrochemical determination of amoxicillin, Electrochim. Acta, 174 (2015) 33–40.

[15] W.J. Liang, Y.H. Lu, N. Li, H.H. Li, F. Zhu, Microwave-assisted synthesis of magnetic surface molecular imprinted polymer for adsorption and solid phase extraction of 4-nitrophenol in wastewater, Microchem. J., 159 (2020) 105316, doi: 10.1016/j.microc.2020.105316.

[16] M.-L. Hu, V. Safarifard, E. Doustkhah, S. Rostamnia, A. Morsali, N. Nouruzi, S. Beheshti, K. Akhbari, Taking organic reactions over metal-organic frameworks as heterogeneous catalysis, Microporous Mesoporous Mater., 256 (2018) 111–127.

[17] P. Kumar, K. Vellingiri, K.-H. Kim, R.J.C. Brown, M.J. Manos, Modern progress in metal-organic frameworks and their composites for diverse applications, Microporous Mesoporous Mater., 253 (2017) 251–265.

[18] H.X. Ou, Q.H. Chen, J.M. Pan, Y.L. Zhang, Y. Huang, X.Y. Qi, Selective removal of erythromycin by magnetic imprinted polymers synthesized from chitosan-stabilized Pickering emulsion, J. Hazard. Mater., 289 (2015) 28–37.

[19] F. Zhu, L.W. Li, J.D. Xing, Selective adsorption behavior of Cd(II) ion imprinted polymers synthesized by microwave-assisted inverse emulsion polymerization: adsorption performance and mechanism, J. Hazard. Mater., 321 (2017) 103–110.

[20] F. Zhu, Y.H. Lu, L.W. Li, Synthesis, adsorption kinetics and thermodynamics of ureido-functionalized Pb(II) surface imprinted polymers for selective removal of Pb(II) in wastewater, RSC Adv., 6 (2016) 111120–111128, doi: 10.1039/C6RA18736F.

[21] L.X. Li, J.F. Yao, P. Xiao, J. Shang, Y. Feng, P.A. Webley, H.T. Wang, One-step fabrication of ZIF-8/polymer composite spheres by a phase inversion method for gas adsorption, Colloid Polym. Sci., 291 (2013) 2711–2717.

[22] N.A. Khan, B.K. Jung, Z. Hasan, S.H. Jhung, Adsorption and removal of phthalic acid and diethyl phthalate from water with zeolitic imidazolate and metal–organic frameworks, J. Hazard. Mater., 282 (2015) 194–200.

[23] H. Jia, M. Marco, G. Ashesh, B. Darren, MOF-polymer composite microcapsules derived from Pickering emulsions, Adv. Mater., 25 (2013) 2717–2722.

[24] K. Chullasat, P. Nurerk, P. Kanatharana, F. Davis, O. Bunkoed, A.B. Chemical, A facile optosensing protocol based on molecularly imprinted polymer coated on CdTe quantum dots for highly sensitive and selective amoxicillin detection, Sens. Actuators, B, 254 (2018) 255–263.

[25] H.Q. Li, J.T. Hu, Y.Y. Cao, X.H. Li, X.J. Wang, Development and assessment of a functional activated fore-modified bio-hydrochar for amoxicillin removal, Bioresour. Technol., 246 (2017) 168–175.

[26] L. Sellaoui, E.C. Lima, G.L. Dotto, A.B. Lamine, Adsorption of amoxicillin and paracetamol on modified activated carbons: equilibrium and positional entropy studies, J. Mol. Liq., 234 (2017) 375–381.

[27] M.A. Chayid, M.J. Ahmed, Amoxicillin adsorption on microwave prepared activated carbon from *Arundo donax* Linn: isotherms, kinetics, and thermodynamics studies, J. Environ. Chem. Eng., 3 (2015) 1592–1601.